Distribution of impurities and minor components in nanostructured conducting oxides

B. Straumal*

Institute of Solid State Physics
Russian Academy of Sciences
Chernogolovka, Moscow Distr.
142432 Russia
and
Moscow State Institute of Steel and Alloys (Technological University)
Leninsky Prospect 4
119991 Moscow, Russia
Fax:+7 495 2382326 E-mail: straumal@issp.ac.ru
*Corresponding author

A. Mazilkin

Institute of Solid State Physics
Russian Academy of Sciences
Chernogolovka, Moscow Distr.
142432 Russia
E-mail: mazilkin@issp.ac.ru

P. Straumal and A. Myatiev

Moscow State Institute of Steel and Alloys (Technological University)
Leninsky Prospect 4
119991 Moscow, Russia
E-mail: Lone5@yandex.ru E-mail: amyatiev@misis.ru

Abstract: Nanostructured conducting oxides are very promising for various applications like varistors (doped zinc oxide), electrolytes for the solid oxide fuel cells (ceria, zirconia, yttria), semi-permeable membranes and sensors (perovskite-type oxides). Grain boundary (GB) phases crucially determine the properties of nanograined-oxides. GB phase transformations (wetting, prewetting, pseudopartial wetting) proceed in the conducting oxides. Novel GB lines appear in the conventional bulk phase diagrams. They can be used for the tailoring of properties of nanograined-conducting oxides, particularly by using the novel synthesis method of liquid ceramics.

Keywords: nanostructures; grain boundaries; conducting oxides; phase transitions.

Reference to this paper should be made as follows: Straumal, B., Mazilkin, A., Straumal, P., and Myatiev, A. (2008) 'Distribution of impurities and minor components in nanostructured conducting oxides', *Int. J. Nanomanufacturing*, Vol. 2, No. 3, pp.253–270.

Biographical notes: Boris Straumal is the Head of the Laboratory for Interfaces in Metals of the Institute of Solid State Physics of Russian Academy of Sciences (RAS) in Chernogolovka, Moscow District, Russia. He is also the Professor of the Department of Physical Chemistry at the Moscow State Institute of Steel and Alloys (Technological University) in Moscow, Russia. He received his DSc in Physics from the same institute of RAS. He worked for many years as a Guest Scientist at the Max-Planck-Institute for Metals Research in Stuttgart, Germany. His interests include phase transformations in low-dimensional solids, coating technologies, and analysis of materials. He is author of four books and more than 200 papers. Citation number: 1303 (18.12.2007).

Andrei Mazilkin is Scientific Associate at the Institute of Solid State Physics of RAS in Chernogolovka, Moscow District, Russia. He received his PhD in Physics from the same institute of RAS. His interests include mechanical properties of nanostructured alloys, phase transformations in solids, electron microscopy, and diffraction methods of analysis.

Peter Straumal is a PhD student at the Department of Physical Chemistry at the Moscow State Institute of Steel and Alloys (Technological University) in Moscow, Russia. He received his MSc in Physics from the same university. His interests include coating technologies, analysis of materials, and synthesis of conducting oxides.

A. Myatiev is the Head of the Laboratory for Nanostructures of the Department of Physical Chemistry at the Moscow State Institute of Steel and Alloys (Technological University) in Moscow, Russia and the Associate Professor of the same department. He received his PhD in Materials Technology at the Baumann University of Technology in Moscow, Russia. His interests include coating technologies, synthesis of conducting oxides for fuel cells, hydrogen storage technologies, and nanostructured materials.

1 Introduction

Conducting oxides are currently broadly used for various applications, for example, zinc oxide for manufacturing of varistors (Wang and Chiang, 1998; Luo et al., 1999), ruthenates as thick-film resistors (Chiang et al., 1994), oxides of fluorite structure (ceria, zirconia, yttria) as electrolytes for the solid oxide fuel cells (SOFC) and oxygen sensors (Duncan and Lasia, 2005), perovskite-type oxides ($BaTiO_3$, $SrTiO_3$, $LaAlO_3$, $LaCrO_3$, etc.) as electrolytes and electrodes for SOFC, semi-permeable membranes and sensors (Park and Cho, 2002). Other applications of semiconducting-oxides are various electronic devices such as self-controlled heaters, colour TV degaussers, fuel evaporators and air-conditioning equipment (Park and Choi, 2002).

The electrical properties of these oxides, especially of nanostructured ones, are crucially determined by the structural and chemical characteristics of the grain boundaries (GBs). It can be due to the formation of:

1 conventional GB segregation layer with a content of a second (third, fourth, etc.) component less than one monolayer (ML)

2 thin (few nm) continuous layer of a GB phase which can be described also as multilayer segregation

3 thick (several μm and more) layer of a solid, liquid or amorphous wetting phase.

Such GB layers may be thermodynamically stable, meta-stable or unstable. Therefore, it is of crucial importance, to have on disposal the phase diagrams including the lines of bulk and GB phase transformations. Such diagrams allow tailoring the synthesis of nanostructured oxides, controlling their microstructure and producing the devices with stable properties and long life-time.

2 GB phase transformations and phase diagrams

Let us consider the schematic two-component eutectic phase diagram describing the conditions for the thermodynamic equilibrium for all three cases listed above. Thermodynamically stable GB layers form as a result of so-called GB phase transitions, GB wetting being an important example of such processes (Chang et al., 1999; Straumal et al., 1997). GB wetting phase transitions have recently been included in the traditional phase diagrams of several systems (Divinski et al., 2005; Schölhammer et al., 2001). The occurrence of wetting depends on the GB energy, σ_{GB}. Consider the contact angle Θ between a bicrystal and a liquid phase. When σ_{GB} is lower than $2\sigma_{SL}$, where σ_{SL} is the energy of the solid/liquid interphase boundary, the GB is non-wetted and $\Theta > 0°$ (point 1 in Figure 1). However, if $\sigma_{GB} \geq 2\sigma_{SL}$, the GB is wetted and the contact angle $\Theta = 0°$ (point 2). The temperature dependence of $2\sigma_{SL}$ is stronger than that of σ_{GB}. If the curves describing the temperature dependencies of σ_{GB} and $2\sigma_{SL}$ intersect, the GB wetting phase transition will occur upon heating at the temperature T_w of their intersection. At $T \geq T_w$ the contact angle is $\Theta = 0°$. By crossing the bulk solidus between points 2 and 3 the liquid phase becomes meta-stable. Its appearance in the system costs the energy loss Δg. The energy gain ($\sigma_{GB} - 2\sigma_{SL}$) above T_w can stabilise the GB liquid-like layer of a thickness l. By moving from point 3 to point 4 the energy loss Δg increases and the GB liquid-like layer disappears at GB solidus line. Therefore, the stable layer of liquid-like phase (which is unstable in the bulk) can exist in the GB between bulk and GB solidus lines (point 3). The same is true also if the second phase is solid. In the point 2' GB in the α-phase has to be substituted by the layer of β-phase and two α/β interphase boundaries (IBs). In the point 3', GB is covered by the equilibrium layer of a β-like phase which is unstable in the bulk. In the points 4 and 4', GB is 'pure' and contains only the usual segregation layer of component B. Therefore:

1 conventional GB segregation layer with a content of a second (third, fourth, etc.) component less than one ML exists in areas marked by points 4 and 4'

2 thin (few nm) continuous layer of a GB phase exists in areas marked by points 3 and 3'

3 thick (several μm and more) continuous GB wetting layer of a liquid or solid phase exists in areas marked by points 2 and 2'.

This simple scheme permits to understand the phenomena in numerous conducting oxides. Very frequently, they are produced with the aid of the liquid phase sintering,

where all GBs are wetted by liquid phase (i.e., in the area 2 of the scheme in Figure 1). By the following cooling, the GB melt layer solidifies and can transform either into array of droplets, or into an amorphous GB layer, or into a crystal wetting phase, or into a conventional GB segregation layer of less than one ML. In details, the GB phases and GB structure in conducting oxides determining their life-time and properties strongly depend on the composition and the processing route.

Figure 1 Schematic phase diagram with lines of GB phase transitions

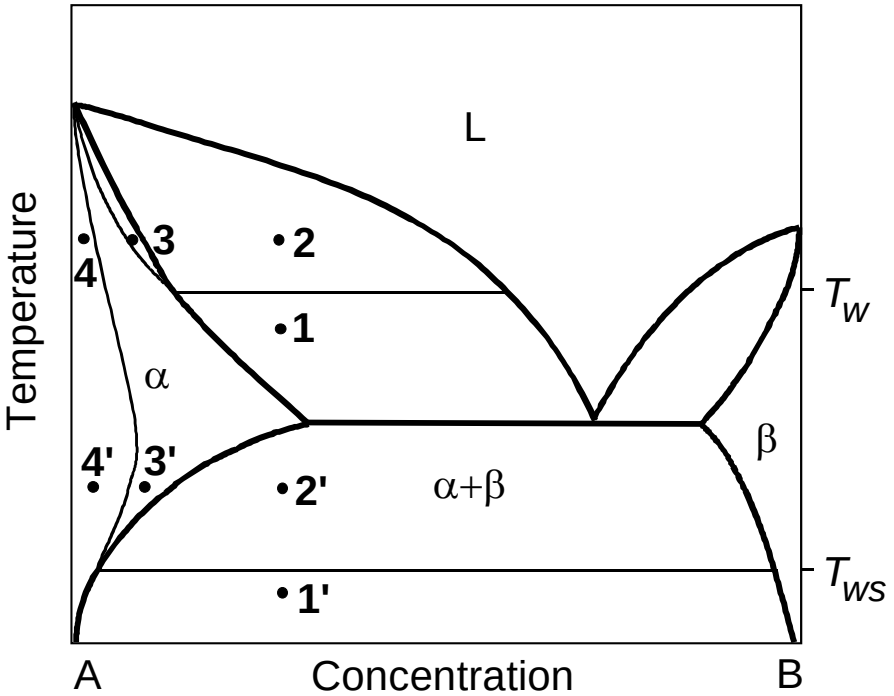

Notes: T_W – temperature of the GB wetting phase transition (proceeds between points 1 and 2). T_{WS} – temperature of the GB solid phase wetting transition (proceeds between points 1' and 2'). Between points 3 and 4 the GB premelting phase transition occurs. Between points 3' and 4' the GB premelting phase transition occurs. In points 3 and 3' GB is covered by the equilibrium layer of a liquid-like or β-like phase which is unstable in the bulk.

3 Grain boundary phases in zinc oxide

Zn oxide is mainly used for manufacturing of varistors. Varistors exhibit highly non-linear current-voltage characteristics with a high resistivity below a threshold electric field, becoming conductive when this field is exceeded, enabling them to be used in current over-surge protection circuits (Matsuoka, 1971). The model usually proposed to account for the electrical properties of ZnO-based varistors is constituted on the basis of a bricklayer. ZnO-based varistors are approximated as a stacking of good conducting grains separated by grain boundaries, which support back-to-back double Schottky barriers

(Levinson and Philipp, 1986; Gupta, 1990; Greuter and Blatter, 1990). Polycrystalline zinc oxide contains small amounts of dopants, mainly bismuth oxide. After liquid-phase sintering such material consists of ZnO grains separated by the Bi_2O_3-rich GB layers. Interfaces between the ZnO grains control the non-linear current-voltage characteristics. Though the Schottky barriers at ZnO/ZnO boundaries mainly control the voltage-dependent resistivity of a varistor, the Bi-rich GB phase also inputs into the overall resistivity.

The inter-granular phase originates from the liquid-phase sintering. The sintering conditions alter the performances of ZnO varistors (Gupta, 1990). An increase in the sintering temperature results usually in a lowering in the nonlinearity of the current-voltage curve. Bhushan et al. pointed out that an increase in the sintering temperature would lower the Schottky barrier height (Bhushan et al., 1981) and Wong mentioned that the volatilisation of Bi_2O_3 during the sintering would bring a loss in the non-ohmic property of the varistors (Wong, 1980). The big amount of structural investigations permitted us to construct the GB lines in the ZnO-Bi_2O_3 bulk phase diagram (Figure 2) (Wang and Chiang, 1998; Luo et al., 2005; Wong, 1974; Wong and Morris, 1974; Greuter, 1995; Gambino et. al., 1989; Kingery et al., 1979; Olsson et al., 1985, Olsson and Dunlop, 1989; Lee et al., 1997). The first variant of the ZnO-Bi_2O_3 phase diagram has been experimentally constructed by Safronov et al. (Safronov et al., 1971). However, recently Guha et al. (2004) found new γ-Bi_2O_3-phase and refined the ZnO-Bi_2O_3 phase diagram (Figure 2).

The liquid phase sintering of the ZnO+Bi_2O_3 mixture proceeds in the ZnO+liquid region of the ZnO-Bi_2O_3 phase diagram, i.e., above eutectic temperature of T_e = 738°C (usually at 850°C) (Wang and Chiang, 1998). During the liquid phase sintering, all ZnO/ZnO GBs are completely wetted by the thick layer of the melt. The thickness of the melt layer is governed only by the grain size and amount of the liquid phase (i.e. on the $Bi2O_3$ content). At 850 °C liquid phase completely wets not only all ZnO/ZnO GBs, but also the free surface of the ZnO particles (Luo et al., 2005). There is some indications that in the ZnO+liquid region close to Te the complete GB wetting transforms into partial GB wetting (with contact angels above zero) (Wang and Chiang, 1998). In other words, in the ZnO-Bi_2O_3 phase diagram the GB wetting tie-line exists slightly above T_e (Figure 2).

The quenching from 850°C leaves a thick inter-granular phase at the ZnO/ZnO GBs. However, the slow cooling below T_e leads to the dewetting of ZnO/ZnO GBs by crystallisation of Bi_2O_3 (Wong, 1974; Wong and Morris, 1974; Gambino et. al., 1989). Since the optimisation of the varistor properties needs the slow cooling or a low-temperature post annealing, much work was devoted to the structure of GBs in varistors (Greuter, 1995; Gambino et. al., 1989; Kingery et al., 1979). At the beginning of these investigations it was believed that all GBs contain thin Bi-rich inter-granular phase. Then Clarke reported that most ZnO-GBs in a commercial varistor were free from the second-phase films, and the atomically abrupt GBs were observed using the lattice fringe imaging (Clarke, 1978). However, later Olsson et al. found the continuous Bi-rich films in the majority of ZnO/ZnO GBs, and only a few GBs were atomically ordered up to the GB plane (Olsson et al., 1985; Olsson and Dunlop, 1989). It was also found that the treatment at high hydrostatic pressure of 1 GPa leads to the desegregation of ZnO/ZnO GBs (Lee et al., 1997). During desegregation the Bi-rich GB phase disappears due to the Bi-GB diffusion towards the secondary phase in the GB triple junctions.

Figure 2 ZnO – Bi_2O_3 phase diagram (solid lines)

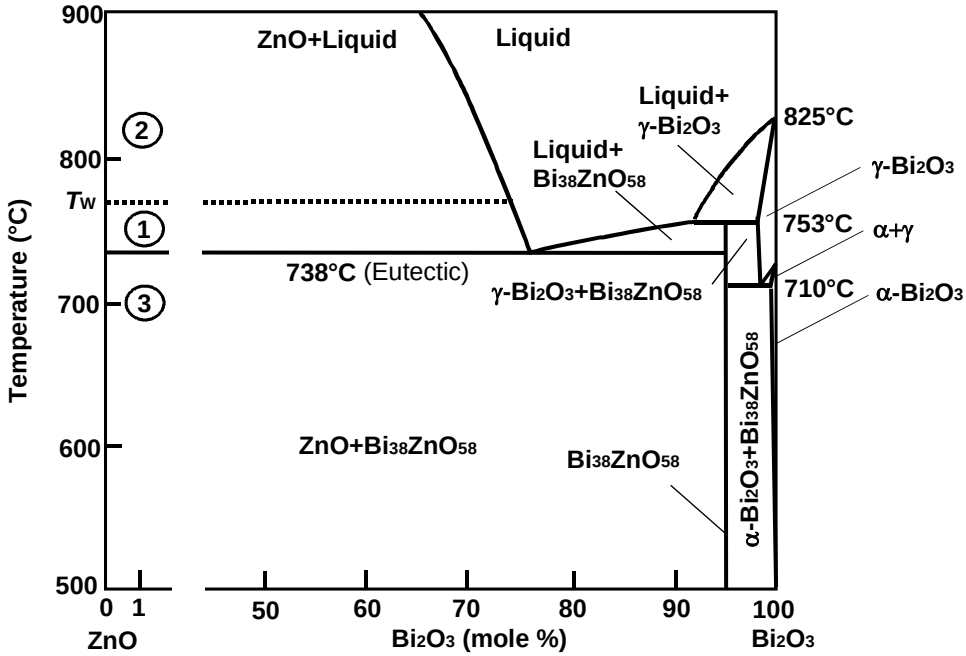

Notes: Tie-line of GB wetting phase transition slightly at T_w above eutectic temperature T_e is added to the bulk diagram (dotted line). In the area (1) between T_e and T_w melt partially wets the ZnO GBs (Wang and Chiang, 1998). In the area (2) above T_w melt fully wets the ZnO GBs (Wang and Chiang, 1998). In the area (3) below T_e ZnO GB triple junctions contain crystalline Bi_2O_3 and ZnO GBs contain amorphous Bi-rich phase with about 25-30 mol. % Bi (see scheme in Figure 3b) (Wang and Chiang, 1998; Luo et al., 2005).

Source: Guha et al. (2004)

Wang and Chiang (1998) studied the ZnO with 0.23 mol. % at Bi_2O_3 700°C. The samples were brought into equilibrium at this temperature from three different starting points:

1 after liquid phase sintering at 850°C followed by 24 h annealing at 700°C and slow cooling down to the room temperature

2 by sintering directly at 700°C (i.e., below T_e, without presence of any liquid phase) for 2 h by 1 GPa followed by the annealing at 700°C at the room pressure

3 equilibrium segregation at 700°C was reached from the high-pressure desegregated state.

Wang and Chiang discovered that in all three cases the equilibrium GB state at 700°C is the amorphous inter-granular film of 1.0–1.5 nm in thickness. In other words, a thin inter-granular film has a lower free energy in comparison with pure crystal-crystal GB. The thermodynamic conditions for the existence of such films were studied by Clarke (1987). After desegregation at high temperature (Figure 3a), GBs are free from any Bi-rich layers (thin or thick). Crystalline Bi_2O_3 particles are present in the GB triple junctions. However, after additional annealing at the same temperature of 700°C but at atmospheric pressure, Bi diffuses back from the triple junctions into the GBs forming the

amorphous GBs films of 1.0–1.5 nm in thickness (Figure 3b). In other words, the amorphous film builds not from the under-cooled liquid, but in the solid phase, as a result of Bi GB diffusion. Moreover, the thin amorphous film covers not only the ZnO/ZnO GBs, but also the interphase boundary between ZnO grains and $Bi2O_3$ particle in the ZnO GB triple junction (Figure 3b).

Figure 3 Scheme of GBs and GB triple junction in the ZnO-Bi_2O_3 at 700°C

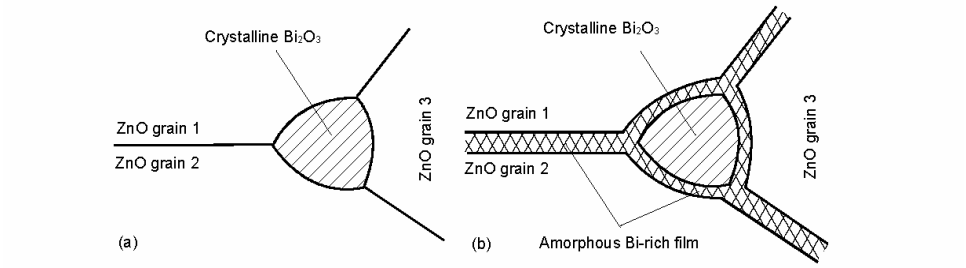

Notes: (a) Structure after pressure desegregation at 1 GPa. GB triple junction contains lenticular crystalline Bi_2O_3 phase. GBs contain no films.
(b) Structure after additional anneal at atmospheric pressure. GBs contain amorphous Bi_2O_3-rich film of 1-2 nm thickness with about 25-30 mol. % Bi. Similar film separates ZnO grains and the lenticular crystalline Bi_2O_3 phase in the GB ZnO triple junction.

Source: Wang and Chiang (1998)

This behaviour can be explained by the so-called pseudopartial wetting (Brochard-Wyart et al., 1991; Luo et al., 2005). At certain thermodynamic conditions, liquid droplets have a non-zero contact angle with a solid substrate (or a GB), but the rest of a substrate surface (or a GB) is not dry, but covered by a thin film of few nm thickness. For example, the liquid Bi-rich nanodroplets (5–15 nm) with contact angle of about 40° were observed on the top of the amorphous film of 1.95 nm thickness on the ZnO surface facets (Luo et al., 2005).

4 Conducting oxides of fluorite structure

Conducting oxides of fluorite structure have received much attention in recent years due to their ionic conductivity with the applications as electrolytes for the SOFC and oxygen sensors. Yttria-stabilised zirconia (YSZ) is by far the most widely used solid electrolyte for technological applications. The main factors driving the interest for this solid electrolyte are its high chemical stability in oxidising or reducing environments and its compatibility with a variety of adjoining electrode materials. It is presently employed at temperatures above 600°C. Other oxides like calcia or scandia can also be used for stabilisation of zirconia. Though stabilised zirconia exhibits good conductivity at high temperatures, however, the need for a better oxygen-conducting material in SOFCs has shifted interest to doped ceria (Tuller et al., 1975; Steele, 2000), which exhibits good conductivity at lower temperatures. Usual doping ions for CeO_2 are Gd^3+, Sm^3+ and Y^3+. Substitution of the Ce^4+ cations in the lattice results in the formation of vacancies and enhances the ionic conductivity.

4.1 GB wetting phases

It has been shown that the maximum of the ionic conductivity of yttria-stabilised zirconia occurs around 9.5 mol. % Y_2O_3 (Filal et al., 1995). Measurements of conductivity and oxygen diffusivity confirmed that YSZ are the ionic conductors at the temperatures as low as 200°C (Petot-Ervas and Petot, 1999). Critical for the low-temperature applications are the internal interface properties of YSZ. In YSZ a glassy phase was frequently observed in GBs and GB triple junctions. In Rizea et al. (2002), two YSZs (called Z_C and Z_F) were sintered from powders prepared through two different processing routes. In samples Z_C, the glassy phase wetted GBs and GB triple junctions. Glassy phase in triple junctions has a shape of stars with zero contact angles at GBs. These 'stars' continue towards GBs as GB wetting layers. In samples Z_F, the amorphous precipitates of glassy phase in triple junctions are lenticular, and spherical glass pockets are widely dispersed in the bulk of grains, but there is no evidence of glassy films at grain boundaries. As a result, the grain boundary conductivity of the Z_F polycrystal, which shows glass-free grain boundaries, is about three orders of magnitude higher than that of the Z_C material (Figure 4). These results are consistent with the mechanism of oxygen-ion transport across grain boundaries suggested by Badwal (1995). Conductivity occurs without any constriction of current pathways in the Z_F ceramics, while it is restricted to the unwetted grain boundaries in the Z_C ceramics. Therefore, if a GB wetting phase is detrimental, one can change a composition in such a way, that the GB wetting conditions are not fulfilled any more. In this case, the GB network of detrimental phase is broken and properties of a material improve. Thus, changing GB wetting conditions by micro-alloying one can improve the properties of a conducting oxide.

Figure 4 Temperature dependence of specific GB conductivity of YSZ polycrystals with and without GB glassy phase according to the data of Rizea et al. (2002)

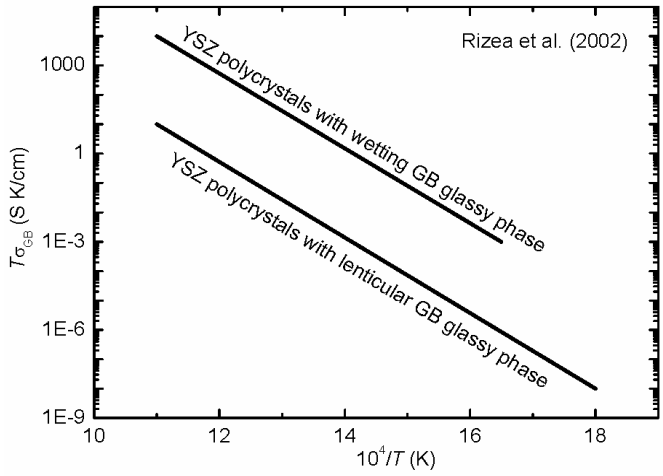

4.2 Monolayer GB segregation

Even in the absence of the GB layers of wetting phases, the properties of conducting oxides can be controlled by the conventional (less that one monolayer) GB segregation.

In the zirconia obtained by the conventional sintering methods a minor amount of silicon, originated from contaminated starting materials, detrimentally influences the conductivity of fuel cells oxides (Aoki et al., 1996). This effect originates from silicon coverage of GBs in stabilised zirconia with formation of a continuous GB network in the polycrystal. Silicon-containing phase form lenticular GB particles and they do not wet the GBs. However, if the Si concentration in GBs reaches about 0.5 monolayer, the GB conductivity drastically decreases, and does not change much with further increase of GB Si content (Aoki et al., 1996). However, if the grain size in stabilised zirconia decreases from micrometer into the nanometer range, the amount of silicon is not more enough to contaminate all GBs. As a result, the specific GB conductivities in nanocrystalline calcia-stabilised zirconia increase about five times (Aoki et al., 1996). The specific GB conductivities of the nanocrystalline YSZ samples (grain size 40 nm) is one to two orders of magnitude higher than that of the microcrystalline samples (grain size 400–1,000 nm) (Figure 5) (Mondal et al., 1999). Therefore, the detrimental effect of Si-contamination vanishes and overall properties of nanostructured zirconia improve. Similar effect of grain size was observed in the scandia-stabilised zirconia (Xu et al., 2004). The specific GB conductivities measured using the impedance spectroscopy increase almost two orders of magnitude when grain size decreases from 6,000 to 60 nm (Figure 5). It is an important example, how the GB engineering (tailoring the polycrystal properties by controlling the GB structure and composition) can improve the properties of nanostructured oxides for fuel cells. Thus, decreasing the grain size, one can dilute the detrimental GB segregation down to the harmless value and improve the properties of a conducting oxide.

Figure 5 Temperature dependence of specific GB conductivity in nano- and microcrystalline zirconia stabilised by yttria and scandia

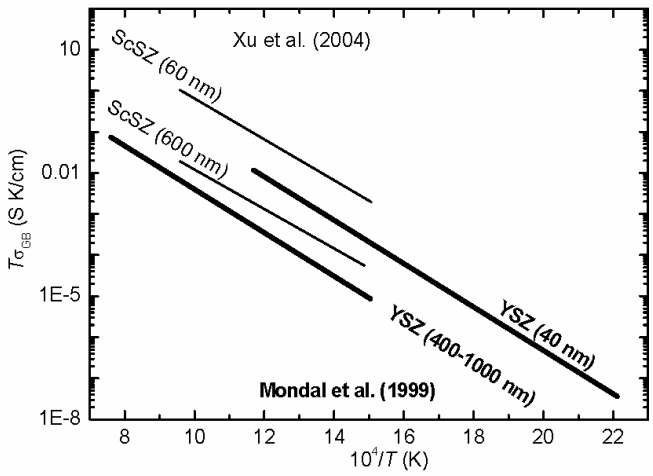

Notes: Specific GB conductivity increases by decreasing grain size. Thick lines represent the data of Mondal et al. (1999) for yttria-stabilised zirconia. Thin lines represent the data of Xu et al. (2004) for scandia-stabilised zirconia.

4.3 Scavengers for GB impurities

Another way to compensate the detrimental Si influence and to improve the GB conductivity in zirconia and ceria is to use the so-called scavengers. It has been shown already in 1982 that small additions of Al_2O_3 drastically improve the ionic conductivity of YSZ (Butler and Drennan, 1982). Later Al_2O_3 was identified as a most effective dopant in increasing the GB conductivity of zirconia-based electrolytes (Godickemier et al., 1994; Feighery and Irvine, 1999; Yuzaki and Kishimoto, 1999; Guo et al., 1995). Butler and Drennan suggested that alumina acts as a 'scavenger' for SiO_2 since the affinity of SiO_2 to Al_2O_3 is greater than to the ZrO_2 (Butler and Drennan, 1982). As a result, the particles of Al_2O_3 present in the ceramic 'sweep-out' silicon from zirconia GBs. It results in the purification effect similar to that of the decrease of grain size. The best scavenger for ceria-based electrolyte is the iron oxide (Zhang et al., 2004).

4.4 Heavy-doping

Figure 6 Bulk (triangles) and total (circles) electrical conductivities at T = 440°C of La- , Y- and Gd- doped microcrystalline cerium oxide as function of dopant concentration according to the data of Tschöpe et al. (2004)

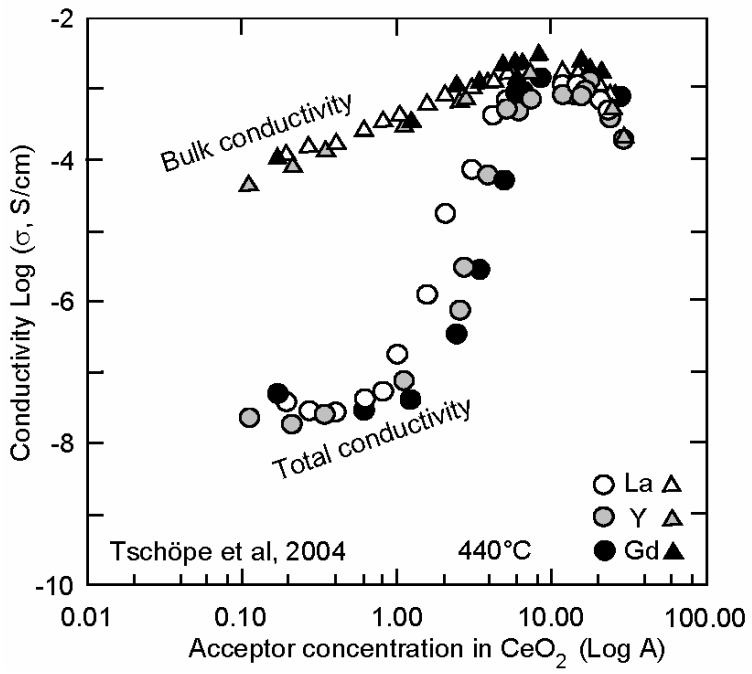

Heavy-doping is another way to change the GB composition and, therefore, improve the conductivity of an oxide. Cerium oxide is a mixed ionic/electronic conductor and exhibits high ionic conductivity when doped with lower valent cations (acceptors). As the oxygen vacancy mobility is even higher than in cubic zirconia – the other prominent fluorite-structured oxygen ion conductor – there has been considerable interest in the potential of ceria-based solid electrolytes for applications in solid oxide fuel cells or

oxygen membranes. In Tschöpe et al. (2004), the microcrystalline ceria was doped with Y, La and Gd in the broad concentration range between 0.1 and 27 at. %. The grain boundary effect, which is indicated by the gap between the bulk and the total conductivity, was found to decrease rapidly as the acceptor concentration increases. The GB conductivity drastically increases at the acceptor concentration between two and ten at. % (Figure 6). Simple estimation reveals that the GB conductivity reaches the bulk value when all GBs become covered with a monolayer of an acceptor impurity (for the ceria grain size of about one μm).

5 GB phenomena in perovskites

Perovskite-type oxides ($BaTiO_3$, $SrTiO_3$, $LaAlO_3$, $LaCrO_3$, etc.) have recently attracted considerable attention for their applications in high-temperature electrochemical devices, such as electrolytes and electrodes of solid oxide fuel cells, oxygen permeating membranes and sensors etc. For the ionic conduction, some perovskites exhibit surprisingly high ionic conductivities, higher than those of well-known zirconia-based materials. The impedance spectroscopy permits to separate bulk and GB inputs in overall conductivity. In many cases the overall conductivity of perovskites is determined by the grain boundary resistance, like for example that of Sr and Mg doped $LaAlO_3$ below 550°C (Park and Choi, 2002). However, the GB input into overall conductivity gradually decreases by increasing temperature. GBs in perovskites mainly contain the conventional GB segregation layer. Only in few cases (like in $BaTiO_3$ sintered from powder particles with Mn coating) the GB amorphous region with a width of about one nm was observed (Park and Cho, 2002). The boundary width in such polycrystals is about five times larger than that in the $BaTiO_3$ sintered from powder particles without Mn coating. The electrostatic potential barrier height of the $BaTiO_3$ ceramics increased from 0.18 to 0.24 eV, due to the increase in the width of the excess negative charge layer from 70 to 120 nm, with increasing the amount of the powder coating material from zero to 1.0 at. %. A systematic variation of the grain boundary features with the amount of coating material indicates the possibility of using this synthesis method to get fine control over the chemistry and electrical properties of the semiconducting $BaTiO_3$ ceramics.

6 Influence of synthesis route on the properties of nanostructured materials

The unique properties of nanostructured materials (including those of nanograined conducting oxides) are of great importance for various advanced applications. However, there are some indications that physical properties of the same material with the same grain size in a nanometer range depends drastically on the preparation technique.

It is well-known that during manufacturing of nanostructured materials the amorphisation may happen, the supersaturated solid solutions may appear, the meta-stable phases may form (Yavari et al., 1992). However, there are indications that physical properties of the same material with the same grain size in a nanometer range depend on the preparation technique. The most reliable data on the formation of meta-stable phases came from ball milling experiments. Particularly, the ball milling of

steels reliably and reproducibly leads to the dissolution of cementite or formation of amorphous solid solution in steels (Xu et al., 2002; Ohsaki et al., 2005; Wang et al., 1995; Campbell et al., 1997). Implantation of carbon ions into iron also produces the strongly non-equilibrium structure in surface layers of samples (Ramos et al., 1989). In other words, ball milling also called mechanical alloying can be compared with a kind of mechanic implantation of one material into another. The high-pressure torsion (HPT, also called compression shear) or deep drawing is principally different from the ball milling. The investigations on HPT of Al-based alloys (Straumal et al., 2004; Mazilkin et al., 2006) demonstrated that HPT or deep drawing lead simultaneously :

1 to the formation of highly non-equilibrium nanometer grain structure

2 to disappearance of non-equilibrium phases and formation of phases which are in equilibrium at the HPT temperature and pressure.

The careful experiments and analysis of previous publications on HPT demonstrates that HPT leads to the grain refinement, but cannot lead to the disappearance of equilibrium phases or formation of non-equilibrium phases. It is the most important difference between HPT and ball milling as two technologies for manufacturing of nanostructured materials. Therefore, the application of various novel techniques for the manufacturing of nanograined conducting oxides is very promising, especially when they permit to synthesise the novel stable GB phases.

7 Synthesis of nanostructured oxides by a 'liquid ceramics' method

Nowadays, the majority of conducting oxides are produced by sintering of oxide powders. The addition of oxides with low melting points as sintering adds is used for liquid-phase sintering. Sintering has several disadvantages; particularly it includes the high temperature synthesis steps and leads to the easy contamination of sintered oxides (especially by silicon). New synthesis technologies would permit to broaden the spectrum of oxides and to produce compounds with properties very promising for the SOFCs and electronic components.

Recently, a novel technology for the deposition of multi-component oxide films from organic precursors (so-called liquid ceramics) has been developed (Myatiev et al., 2005). The films can be deposited on various substrates. The deposited films of ZnO, Y_2O_3 and Ce-Gd-Ni complex oxide are dense, non-porous, nanostructured, uniform, non-textured (Figures 7 to 10). Grain size in these films can vary from five to 100 nm. The components in multi-component films are distributed uniformly. This technology is extremely flexible. It allows to synthesise oxides of various compositions and also to change the composition of oxides in the very broad interval. The possibility of tailoring the oxide doping allows one to develop the new advanced materials for the fuel cells and to reach the previously unattainable parameters of the fuel cells. Liquid ceramics method permits to change the grain size and influence the shape of grains (for example, from equiaxial, Figure 9, to pancake-like, Figure 10).

Figure 7 Bright field high-resolution electron micrograph of the nanograined ZnO thin film deposited by the liquid ceramics technology

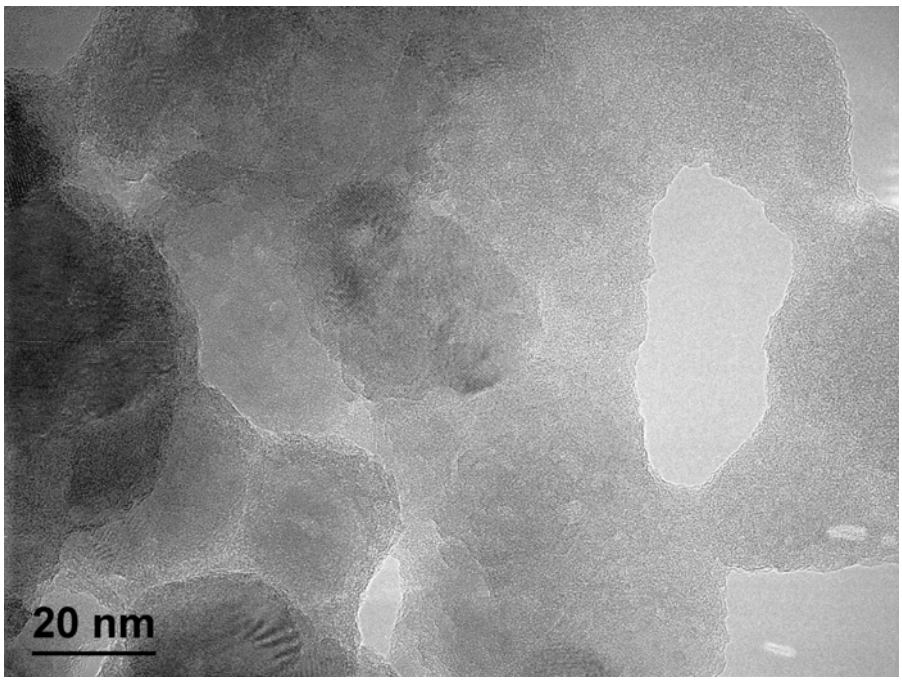

The method of liquid ceramics allows one to intentionally dope the material, particularly the nanograined-oxides containing the high amount of GBs. Another advantage of this method, in comparison with conventional powder metallurgy methods for oxide synthesis, is that the technology step is excluded when the very fine powder particles have the free surface which is able to accumulate various contaminations. Therefore, the deposition of nanostructured-oxides using the organic precursors (liquid ceramics) excludes the uncontrollable contamination of the material. The liquid ceramics method allows to avoid the detrimental impurities, on the one hand, and, on the other hand, to introduce the advantageous doping components which can improve the properties of nanostructured-conductive oxides for fuel cells. The oxides obtained by the liquid ceramics method can be used also for other applications, for example for gas sensors, semiconductor devices (like varistors), advanced medicaments or cosmetic products.

Figure 8 Electron diffraction pattern from the ZnO sample shown in Figure 7 (No texture is visible)

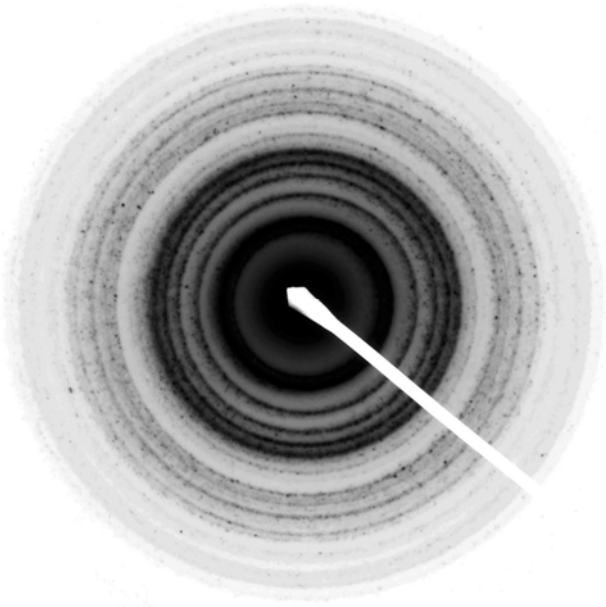

Figure 9 Bright field high-resolution electron micrograph of the nanograined Ce-Gd-Ni complex oxide thin film deposited by the liquid ceramics technology

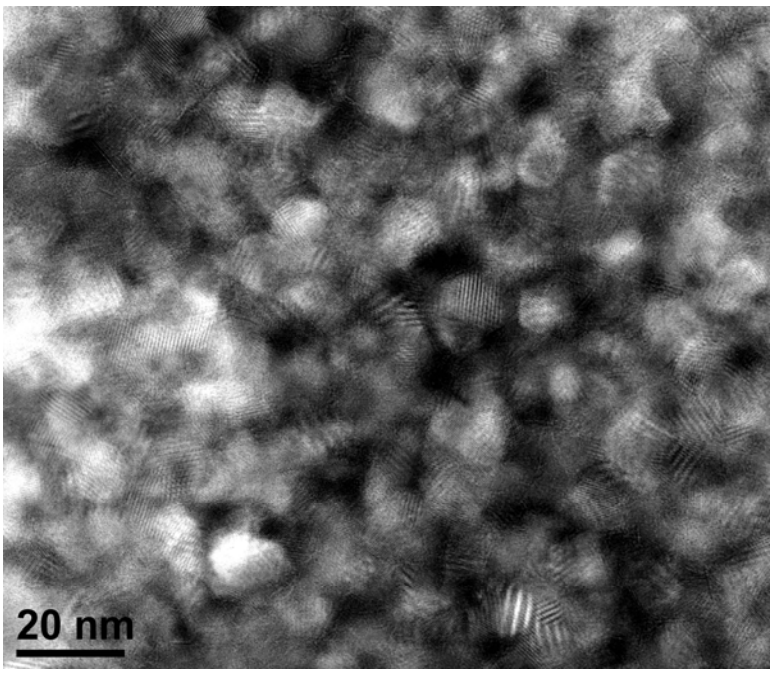

Figure 10 Bright field high-resolution electron micrograph of the nanograined Y_2O_3 thin film deposited by the liquid ceramics technology

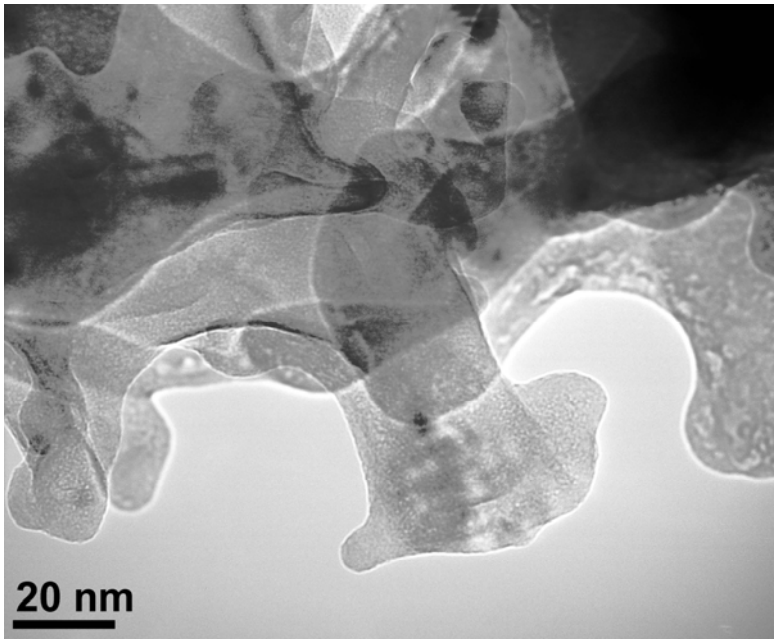

8 Summary

Nanostructured-conducting oxides are very promising for various electronic and energy consumption applications like varistors, electrolytes for the solid oxide fuel cells, semi-permeable membranes and sensors. GB phases crucially determine the properties of nanograined-oxides produced by powder sintering. GB phase transformations (wetting, prewetting, pseudopartial-wetting, etc.) proceed in the conducting oxides during sintering and following thermal treatments. Novel GB lines appearing in the conventional bulk phase diagrams permit the GB engineering and tailoring the properties of nanograined-conducting oxides. Particularly useful are the novel synthesis methods for conducting oxides, like that of liquid ceramics.

Acknowledgements

The authors thank the Russian Foundation for Basic Research (Contracts 06-03-32875 and 08-08-90105) and German Academic Exchange Service. They also greatly appreciate Dr. W. Sigle and Dr. F. Phillipp (Max-Planck-Institut für Metallforschung, Stuttgart, Germany) for their help in the electron microscopy investigations.

References

Aoki, M., Chiang, Y., Kosacki, I., Lee, L.J., Tuller, H., and Liu, Y. (1996) 'Solute segregation and grain-boundary impedance in high-purity stabilised zirconia'. *Journal of the American Ceramic Society*, Vol. 79, pp.1169–1180.

Badwal S.P.S. (1995) 'Grain boundary resistivity in zirconia-based materials: effect of sintering temperatures and impurities', *Solid State Ionics*, Vol. 76, pp.67–80.

Bhushan, B., Kashyap, S.C., and Chopra, K.L. (1981) 'Electrical and dielectric behaviour of a zinc-oxide composite', *Journal of Applied Physics*, Vol. 52, pp.2932–2936.

Brochard-Wyart, F.; di Meglio, J-M.; Quéré, D., and de Gennes, P.G. (1991) 'Spreading of nonvolatile liquids in a continuum picture', *Langmuir*, Vol. 7, pp.335–338.

Butler, E .P. and Drennan, J. (1982) 'Microstrutural analysis of sintered high-conductivity zirconia with Al_2O_3 additives', *Journal of the American Ceramic Society*, Vol. 65, pp.474–478.

Campbell, S.J., Wang, G.M., Calka, A. and Caczmarek, W.F. (1997) 'Ball milling of Fe_{75}-C_{25}: formation of Fe_3C and Fe_7C_3', *Materials Science and Engineering A*, Vol. 226–228, pp.75–79.

Chang, L-S., Rabkin, E., Straumal, B.B., Baretzky, B., and Gust, W. (1999) 'Thermodynamic aspects of the grain boundary segregation in Cu(Bi) alloys', *Acta Materialia*, Vol. 47, pp.4041–4046.

Chiang, Y-M., Silverman, L.A., French, R.H. and Cannon, R.M. (1994) 'Thin glass film between ultrafine conductor particles in thick-film resistors', *Journal of the American Ceramic Society*, Vol. 77, pp.1143–1152.

Clarke, D.R. (1978) 'The microstructural location of the intergranular metal oxide phase in a zinc oxide varistor', *Journal of Applied Physics*, Vol. 49, pp.2407–2411.

Clarke, D.R. (1987) 'On the equilibrium thickness of intergranular glass phases in ceramic materials', *Journal of the American Ceramic Society*, Vol. 70, pp.15–22.

Divinski, S.V., Lohmann, M., Herzig, Chr., Straumal, B., Baretzky, B., and Gust, W. (2005) 'Grain boundary melting phase transition in the Cu–Bi system', *Physical Review B*, Vol. 71, pp.1041041-1–104104-8.

Duncan, H. and Lasia, A. (2005) 'Influence of the electrode nature on conductivity measurements of gadolinia-doped ceria', *Solid State Ionics*, Vol. 176, pp.1429–1437.

Feighery, A.J. and Irvine, J.T.S. (1999) 'Effect of alumina additions upon electrical properties of 8 mol. % yttria-stabilised zirconia', *Solid State Ionics*, Vol. 121, pp.209–216.

Filal, M., Petot, C., Mokchah, M., Chateau, C. and Charpentier, J.L. (1995) 'Ionic conductivity of yttrium-doped zirconia and the 'composite effect', *Solid State Ionics*, Vol. 80, pp.27–35.

Gambino, J.P., Kingery, W.D., Pike, G.E., and Philipp, H.R. (1989) 'Effect of heat treatments on the wetting behavior of bismuth rich intergranular phases in ZnO:Bi:Co varistors', *Journal of the American Ceramic Society*, Vol. 72, pp.642–645.

Godickemier, M., Michel, B., Orlinkas, A., Bohac, P., Sasaki, K., Gauckler, L., Henrich, H., Schwander, P., Kostorz, G., Hofmann, H., and Frei, O. (1994) 'Effect of intergranular glass films on the electrical conductivity of 3Y-TZP', *Journal of Materials Research*, Vol. 9, pp.1228–1240.

Greuter, F. (1995) 'Electrically active interfaces in ZnO varistor', *Solid State Ionics*, Vol. 75, pp.67–78.

Greuter, F. and Blatter, G. (1990) 'Electrical properties of grain boundaries in polycrystalline compound semiconductors', *Semiconductor Science and Technology*, Vol. 5, pp.111–137.

Guha, J.P., Kunej, S., and Suvorov, D. (2004) 'Phase equilibrium relations in the binary system Bi_2O_3-ZnO', *Journal of Materials Science*, Vol. 39, pp.911–918.

Guo, X., Tang, C.Q., and Yuan, R.Z. (1995) 'Grain boundary ionic conduction in zirconia-based solid electrolyte with alumina addition', *Journal of the European Ceramic Society*, Vol. 15, pp.25–32.

Gupta, T.K. (1990) 'Application of zinc oxide varistors', *Journal of the American Ceramic Society*, Vol. 73, pp.1817–1840.

Kingery, W.D., van der Sande, J.B., and Mitamura, T. (1979) 'A scanning transmission electron microscopy investigation of grain boundary segregation in a ZnO–Bi_2O_3 varistor', *Journal of the American Ceramic Society*, Vol. 62, pp.221–222.

Lee, J-R., Chiang, Y-M., and Ceder, G. (1997) 'Pressure-thermodynamic study of grain boundaries: Bi segregation in ZnO', *Acta Materialia*, Vol. 45, pp.1247–1257.

Levinson, L.M. and Philipp, H.R. (1986) 'Zinc-oxide varistors – a review', *American Ceramic Society Bulletin*, Vol. 65, pp.639–646.

Luo, J., Wang, H., and Chiang, Y-M. (1999) 'Origin of solid-state activated sintering in Bi_2O_3-doped ZnO', *Journal of the American Ceramic Society*, Vol. 82, pp.916–920.

Luo, J., Chiang, Y-M., and Cannon, R.M. (2005) 'Nanometer-thick surficial films in oxides as a case of prewetting', *Langmuir*, Vol. 21, pp.7358–7365.

Matsuoka, M. (1971) 'Nonohmic properties of zinc oxide resistors', *Japanese Journal of Applied Physics*, Vol. 10, pp.736–738.

Mazilkin, A.A., Straumal, B.B., Rabkin, E., Baretzky, B., Enders, S., Protasova, S.G., Kogtenkova, O.A., and Valiev, R.Z. (2006) 'Softening of nanostructured Al–Zn and Al–Mg alloys after severe plastic deformation', *Acta Materialia*, Vol. 54, pp.3933–3939.

Mondal, P., Klein, A., Jaegermann, W., and Hahn, H. (1999) 'Enhanced specific grain boundary conductivity in nanocrystalline Y_2O_3-stabilised zirconia', *Solid State Ionics*, Vol. 118, pp.331–339.

Myatiev, A.A., Diachenko, N.I., Pomadchik, A.L., and Straumal, P.B. (2005) 'Synthesis of nanocrystalline oxides Ce_{1-x}–Bi_x–O_y', *Nano- and Microsystem Technology*, Vol. 3, pp.19–25 (in Russian).

Ohsaki, S., Hono, K., Hidaka, H., and Takaki, S. (2005) 'Characterisation of nanocrystalline ferrite produced by mechanical milling of pearlitic steel', *Scripta Materialia*, Vol. 52, pp.271–276.

Olsson, E., Falk, L.K.L., and Dunlop, G.L. (1985) 'The microstructure of a ZnO varistor material', *Journal of Materials Science*, Vol. 20, pp.4091–4098.

Olsson, E. and Dunlop, G. L. (1989) 'Characterisation of individual interfacial barriers in a ZnO varistor material', *Journal of Applied Physics*, Vol. 66, pp.3666–3675.

Park, J.Y. and Choi, G.M. (2002) 'Electrical conductivity of Sr and Mg doped $LaAlO_3$', *Solid State Ionics*, Vol. 154–155, pp.535–540.

Park, M-B. and Cho, N-H. (2002) 'Chemical and structural features of the grain boundaries in semiconducting $BaTiO_3$ ceramics prepared from surface-coated powders', *Solid State Ionics*, Vol. 154–155, pp.407–412.

Petot-Ervas, G. and Petot, C. (1999) 'Experimental procedure for the determination of diffusion coefficients in ionic compounds – application to yttrium-doped zirconia', *Solid State Ionics*, Vol. 117, pp.27–39.

Ramos, S.M.M., Amarai, L., Behar, M., Marest, G., Vasques, A., and Zawislak, F.C. (1989) 'Dissolution and reprecepitation of carbonitride precipitates in a low-carbon steel by an irradiation', *Radiation Effects and Defects in Solids*, Vol. 110, pp.355–365.

Rizea, A., Chirlesan, D., Petot, C., and Petot-Ervas, G. (2002) 'The influence of alumina on the microstructure and grain boundary conductivity of yttria-doped zirconia', *Solid State Ionics*, Vol. 146, pp.341–353.

Safronov, M., Batog, V.N., Stepanyuk, T.V., and Fedorov, P.M. (1971) 'Equilibrium diagram of the bismuth oxide-zinc oxide system', *Russian Journal of Inorganic Chemistry*, Vol. 16, pp.460–466.

Schölhammer, J., Baretzky, B., Gust, W., Mittemeijer, E., and Straumal B. (2001) 'Grain boundary grooving as an indicator of grain boundary phase transformations', *Interface Science*, Vol. 9, pp.43–53.

Steele, B.C.H. (2000) 'Appraisal of $Ce_{1-y}Gd_yO_{2-y/2}$ electrolytes for IT-SOFC operation at 500°C', *Solid State Ionics*, Vol. 129, pp.95–110.

Straumal, B., Rabkin, E., Lojkowski, W., Gust, W. and Shvindlerman, L.S. (1997) 'Pressure influence on the grain boundary wetting phase transition in Fe-Si alloys', *Acta Materialia*, Vol. 45, pp.1931–1940.

Straumal, B.B., Baretzky, B., Mazilkin, A.A., Phillipp, F., Kogtenkova, O.A., Volkov M.N., and Valiev, R.Z. (2004) 'Formation of nanograined structure and decomposition of supersaturated solid solution during high pressure torsion of Al–Zn and Al–Mg', *Acta Materilaia*, Vol. 52, pp.4469–4478.

Tschöpe, A., Kilassonia, S., and Birringer, R. (2004) 'The grain boundary effect in heavily doped cerium oxide', *Solid State Ionics*, Vol. 173, pp.57–61.

Tuller, H.L. and Nowick, A.S. (1975) 'Doped ceria as a solid oxide electrolite', *Journal of the Electrochemical Society*, Vol. 122, pp.255–259.

Wang, G.M., Campbell, S.J., Calka, A. and Caczmarek, W.F. (1995) 'Comparison of the characteristics of nanocrystalline ferrite in Fe-0.89C steels with pearlite and spheroidite structure produced by ball milling', *NanoStructured Materials*, Vol. 6, pp.389–392.

Wang, H. and Chiang, Y-M. (1998) 'Thermodynamic stability of intergranular amorphous films in bismuth-doped zinc oxide', *Journal of the American Ceramic Society*, Vol. 81, pp. 89–96.

Wong, J. (1974) 'Nature of intergranular phase in non-ohmic ZnO ceramics containing 0.5 mol. % Bi_2O_3', *Journal of the American Ceramic Society*, Vol. 57, pp.357–359.

Wong, J. (1980) 'Sintering and varistor characteristics of ZnO–Bi_2O_3 ceramics', *Journal of Applied Physics*, Vol. 51, pp.4453–4459.

Wong, J. and Morris, W.G. (1974) 'Microstructure and phases in non-ohmic ZnO-Bi_2O_3 ceramics', *American Ceramic Society Bulletin*, Vol. 53, pp.816–820.

Xu, G., Zhang, Y.W., Liao, C.S. and Yan, C.H. (2004) 'Grain size-dependent electrical conductivity in scandia-stabilised zirconia prepared by a mild urea-based hydrothermal method', *Solid State Ionics*, Vol. 166, pp.391–396.

Xu, Y., Umemoto, M., and Tsuchiya, K. (2002) 'Comparison of the characteristics of nanocrystalline ferrite in Fe-0.89C steels with pearlite and spheroidite structure produced by ball milling', *Materials Transactions*, Vol. 9, pp.2205–2212.

Yavari, A.R., Desré, P.J. and Benameur T. (1992) 'Mechanically driven alloying of immiscible elements', *Physical Review Letters*, Vol. 68, pp.2235–2238.

Yuzaki, A. and Kishimoto, A. (1999) 'Effects of alumina dispersion on ionic conduction of toughened zirconia base composite', *Solid State Ionics*, Vol. 116, pp.47–51.

Zhang, T.S., Ma, J., Kong, L.B., Chan, S.H., Hing, P., and Kilner, J.A. (2004) 'Iron oxide as an effective sintering aid and a grain boundary scavenger for ceria-based electrolytes', *Solid State Ionics*, Vol. 167, pp. 203–207.